Centennial changes in the heliospheric magnetic field and open solar flux: The consensus view from geomagnetic data and cosmogenic isotopes and its implications

M. Lockwood[1,2] and M. J. Owens[1]

Received 17 October 2010; revised 12 January 2011; accepted 21 January 2011; published 21 April 2011.

[1] Svalgaard and Cliver (2010) recently reported a consensus between the various reconstructions of the heliospheric field over recent centuries. This is a significant development because, individually, each has uncertainties introduced by instrument calibration drifts, limited numbers of observatories, and the strength of the correlations employed. However, taken collectively, a consistent picture is emerging. We here show that this consensus extends to more data sets and methods than reported by Svalgaard and Cliver, including that used by Lockwood et al. (1999), when their algorithm is used to predict the heliospheric field rather than the open solar flux. One area where there is still some debate relates to the existence and meaning of a floor value to the heliospheric field. From cosmogenic isotope abundances, Steinhilber et al. (2010) have recently deduced that the near-Earth IMF at the end of the Maunder minimum was 1.80 ± 0.59 nT which is considerably lower than the revised floor of 4nT proposed by Svalgaard and Cliver. We here combine cosmogenic and geomagnetic reconstructions and modern observations (with allowance for the effect of solar wind speed and structure on the near-Earth data) to derive an estimate for the open solar flux of $(0.48 \pm 0.29) \times 10^{14}$ Wb at the end of the Maunder minimum. By way of comparison, the largest and smallest annual means recorded by instruments in space between 1965 and 2010 are 5.75×10^{14} Wb and 1.37×10^{14} Wb, respectively, set in 1982 and 2009, and the maximum of the 11 year running means was 4.38×10^{14} Wb in 1986. Hence the average open solar flux during the Maunder minimum is found to have been 11% of its peak value during the recent grand solar maximum.

Citation: Lockwood, M., and M. J. Owens (2011), Centennial changes in the heliospheric magnetic field and open solar flux: The consensus view from geomagnetic data and cosmogenic isotopes and its implications, *J. Geophys. Res.*, *116*, A04109, doi:10.1029/2010JA016220.

1. Introduction

[2] Geomagnetic activity can be used to study past variations in the near-Earth heliosphere because it depends mainly on a combination of the IMF field strength, B, the solar wind speed V and the IMF orientation (particularly in the ZY plane of the Geocentric Solar Magnetospheric reference frame) (see review by *Finch and Lockwood* [2007]). The orientation factor becomes constant when averaged over a sufficient interval (e.g., 1 year) [*Stamper et al.*, 1999; *Finch and Lockwood*, 2007]. Thus the reconstruction techniques based annual data need to separate the effects of variations in B and V. *Lockwood et al.* [1999, hereafter LEA99] achieved this by quantifying an expected connection between V and a combination of the level and the solar rotation recurrence of geomagnetic activity. On the other hand, *Svalgaard and Cliver* [2005, 2010] found their IDV geomagnetic index to be predominantly dependent on B alone. *Rouillard et al.* [2007, hereafter REA07] and *Lockwood et al.* [2009a, hereafter LEA09] exploited the observation by *Svalgaard and Cliver* [2007] that different geomagnetic indices respond differently to different combinations of B and V.

[3] *Svalgaard and Cliver* [2010, hereafter SC10] recently updated their IDV geomagnetic index and used it to evaluate the variation of B between 1835 and the present day, based on the extremely good correlation between B and IDV. They review other reconstructed variations of B from historic proxy data and show those by *Svalgaard and Cliver* [2005], REA07 and LEA09 are remarkably similar despite the use of different data and diverse reconstruction methods. SC10 also show a variation in B attributed to LEA99 which appears divergent from the others. In fact, LEA99 did not predict the variation of B, rather they computed that in the open solar flux, F_S. In this paper, we show that the method used by LEA99 also predicts a variation in B that is close to the other reconstructions when it is applied to B rather than Fs. This is a useful addition because the reconstruction method of LEA99 is considerably different from the others in that it uses a different form of the data (range indices only rather than hourly means or a

[1]Space Environment Physics Group, Department of Meteorology, University of Reading, Reading, UK.
[2]Space Science and Technology Department, Rutherford Appleton Laboratory, Chilton, UK.

0148-0227/11/2010JA016220

combination of both) and from different stations. In this paper, section 2 reviews why open solar flux F_S is not simply related to IMF field strength B; section 3 surveys the various reconstructions of B and presents the results of applying the LEA99 procedure to B for the first time; section 4 studies the uncertainties for the reconstruction by SC10 (which is chosen because their algorithm allows relatively straightforward analysis of the error propagation); section 5 compares the different reconstructions of open solar flux, considering the different methods of allowing for small-scale heliospheric structure; section 6 studies the implications of the growing agreement between reconstructions based on geomagnetic activity and cosmogenic isotopes, in particular for estimates of a floor to the IMF field strength; lastly, section 7 estimates the open solar flux at the end of the Maunder minimum.

2. Why Are Open Solar Flux F_S and Near-Earth IMF B Not Simply Related?

[4] The IMF field strength B is a local heliospheric parameter. It has been routinely measured by interplanetary spacecraft at various locations in the heliosphere [*Owens et al.*, 2008], particularly by craft in near-Earth space. On the other hand, the (signed) open solar flux F_S is a global parameter, being the total magnetic flux (of one polarity) leaving the top of the solar atmosphere. The two are related but there are differences between them, dependent on variable processes occurring between the top of the solar atmosphere and the location in the heliosphere considered.

[5] To clarify the differences between B and F_S, it is important to note that estimates of the open solar flux from spacecraft data are possible only because of the finding by the Ulysses spacecraft that the mean of the modulus of the radial heliospheric field component $\langle |B_r|_t \rangle_T$ is independent of heliographic latitude. The averaging must be done over a timescale T that is long enough for longitudinal structure to be averaged out. The timescale t is that on which radial field observations B_r are preaveraged before the absolute value is taken. Because B_r can have either polarity ($B_r > 0$ in "away" sectors and $B_r < 0$ in "toward" sectors), employing a larger t causes toward and away field to cancel to a greater extent within each preintegration period (as the sampling of the two polarities becomes more balanced) and $|B_r|_t$ is reduced. The argument used to justify the use of a single value of t is that it must be large enough to smooth out small-scale structure in the heliospheric field (which arises in the heliosphere and so does not reflect changes in the solar source field) but not so large that variations which do reflect structure in the solar source field are also averaged out. A value of $t = 1$ day has generally been adopted as it makes open solar flux estimates from in situ magnetometer observations match those derived from remote-sensing solar magnetograph data using the Potential Field Source Surface (PFSS) method [*Wang and Sheeley*, 1995; *Lockwood et al.*, 2006].

[6] Because of the Ulysses result that $\langle |B_r|_t \rangle_T$ is independent of heliographic latitude, the (signed) open solar flux from measurements of B_r at a heliocentric distance r is:

$$F_S = \left(4\pi r^2\right) \langle |B_r|_t \rangle_T / 2 = \left(2\pi r^2\right) \langle |B_r|_t \rangle_T \quad (1)$$

Note that the value of $|B_r|_t$, and hence that of F_S derived using equation (1), depends on the value of t used [*Lockwood et al.*, 2006, 2009b]. On the other hand, B can only be positive and so t has no effect on it (after the initial combination of very high time resolution component data has been implemented according to the instrument calibration procedures). Thus a conversion between F_S and B will necessarily depend on the t used [*Lockwood et al.*, 2006].

[7] In order to convert F_S into B (or vice versa) one also needs a relationship between $|B_r|$ and B. As pointed out by *Lockwood et al.* [2006], Parker spiral theory of the frozen-in IMF predicts that as the solar wind speed V increases, the IMF spiral unwinds and so the ratio $|B_r|/B$ increases. Reconstructions by *Svalgaard and Cliver* [2007], REA07 and LEA09 all show that the means of both V and B increased over the past 150 years, from which the theory predicts an increase in the ratio $|B_r|/B$. Thus Parker spiral theory predicts that the fractional increase in $|B_r|$ (and hence F_S) over this interval will have been larger than that in B.

[8] However, this is not the only reason why F_S and B are not simply related. Any longitudinal structure in the solar wind also alters the ratio $|B_r|/B$. For example *Riley and Gosling* [2007] have shown that events of near-radial IMF ($|B_r|/B$ approaching unity) reported by *Jones et al.* [1998] are explained by the kinematic (time-of-flight) effect on the frozen-in field within rarefaction regions where the solar wind velocity decays. *Lockwood et al.* [2009b] have allowed for these kinematic effects in both compression and rarefaction regions and shown that, for a fixed level of open solar flux F_S, both B_r and B are increased by enhanced longitudinal structure in the solar wind flow speed. *Lockwood et al.* [2009b] showed that the observation by *Owens et al.* [2008] that $|B_r|/r^2$ increased with radial distance r (the "excess flux effect") was also consistent with the difference between observations at $r = 1$AU and values deduced from solar magnetograms using the PFSS method. They also showed that the commonly used procedure of preaveraging B_r over 1 day before taking absolute values ($t = 1$ day) was, effectively, an approximate way of making an allowance for the kinematic excess flux effect at $r \leq 1$AU. Note that application of the Ulysses result (equation (1)) was shown to be accurate to within a few percent for $T > 27$ days by *Lockwood et al.* [2004], but even more accurate when the kinematic effect, and its latitudinal variation, is allowed for [*Lockwood and Owens*, 2009]. There are additional factors which may also influence the difference between PFSS and in situ estimates of open flux. These include the calibration of magnetograph data and the limitations of the PFSS method. In particular, *Yeates et al.* [2010] have recently used a non-potential model to show that allowing for currents in the corona increases open flux estimates, particularly at sunspot maximum.

[9] The method of LEA99 derived an expression for F_S as a function of the *aa* geomagnetic activity index from 3 separate correlations. The first two correlations yielded a functional form

$$B = \left[aa / \left\{ k_1 M_E^{2/3} \left(s_f I^{\beta} aa^{\lambda} + c_f \right) \right\} \right]^{-2\alpha} \quad (2)$$

where α, k_1, s_f, c_f, β and λ are fit coefficients and M_E is the Earth's magnetic dipole moment. In addition, they employed $\langle |B_r|_t \rangle_T = s_b B$ (which they noted was only approximately valid but was used instead of the more general $\langle |B_r|_t \rangle_T = s_b B + c_a$

Table 1. Comparison of Best Fit Parameters for the Fit to Open Solar Flux, F_S, in the Paper by *Lockwood et al.* [1999] and for the Fit (Using the Same Procedure) to the Near-Earth IMF Field Strength, B, Presented Here

	Fit to F_S Using Equation (3)	Fit to B Using Equation (2)
s_b	0.561	not applicable
λ	1.303	1.177
β	0.263	0.183
α	0.386	0.533
k_1	5.317×10^{-17}	3.448×10^{-17}
s_f	2.607×10^{4}	2.758×10^{4}
c_f	1.893×10^{6}	1.491×10^{6}

to keep the number of fit parameters to a minimum). Combining this with equations (1) and (2) yields

$$F_s = (2\pi r^2) s_b \left[aa / \left\{ k_1 M_E^{2/3} (s_f I^\beta aa^\lambda + c_f) \right\} \right]^{-2\alpha} \quad (3)$$

To evaluate the coefficients s_b, α, k_1, s_f, c_f, β and λ, LEA99 carried out a single end-to-end fit to F_S (derived from B_r observations using equation (1) with t = 1 h and T = 1 year) using equation (3) with the Nelder-Mead simplex (direct search) method to minimize the r.m.s. residuals [*Nelder and Mead*, 1965; *Lagarias et al.*, 1998]. Note that the same coefficients would not apply in equation (2) to computing B because of the use of the simplified expression $\langle |B_r| \rangle_T = s_b B$ in deriving the fitted functional form.

[10] SC10 used the approximation $B_r = s_b B$ to convert the LEA99 estimates of F_S into the B variation that they show as an orange line in Figure 12 of their paper (marked LEA99) (L. Svalgaard, private communication, 2010). However, because the F_S variation was actually a fit to observed F_S values (from observed IMF B_r), adopting $B_r = s_b B$ in this context does not generate a B variation that is consistent with LEA99's F_S variation.

3. What Does the LEA99 Procedure Give if Applied to *B*?

[11] LEA99 did not apply their procedure to B so it is interesting to ask what they would have obtained had they done so, and how well it agrees with the consensus view described by SC10. We here refit the observations of B using the functional form given in equation (2). Table 1 contrasts the coefficients in the fit to F_S using equation (3), as carried out by LEA99 and those for the variation for B derived here. In addition, the method is applied to the corrected aa index, aa_C, as used by REA07 and LEA09. The derived variation is shown by the orange line in Figure 1. Also shown in this plot, (in blue) is one of the four reconstructions by REA07 and (in red) that by LEA09. The thin black line is that by SC10 and is surrounded by a gray area which is the uncertainty band on that reconstruction (the computation of which is described in section 4). The solid dots are the annual means of the observed B during the space age. The degree of agreement is considerable, especially considering the diversity of data and methods employed, which are summarized here:

[12] SC10 is based on a correlation of the daily IDV index with B, where IDV is derived on a daily basis from hourly mean geomagnetic data from all available stations for 1835 to

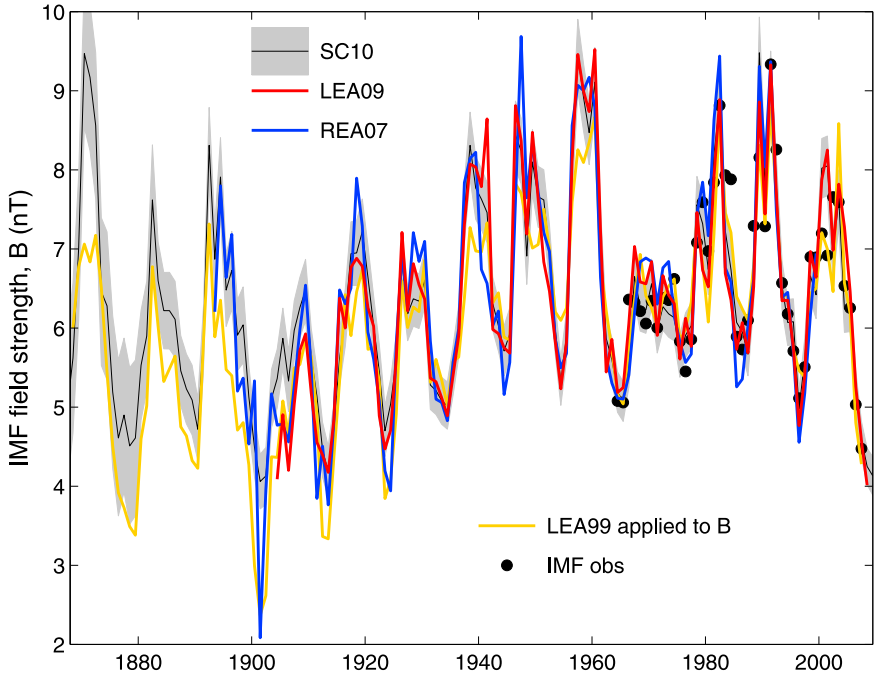

Figure 1. Reconstructions of the near Earth IMF field strength B from geomagnetic activity data. The orange line (LEA99) is that derived in the present paper using the procedure of *Lockwood et al.* [1999], applied to observations of B. The red and blue lines are the reconstructions presented by *Lockwood et al.* [2009a] (LEA09) and *Rouillard et al.* [2007] (REA07). The thin surrounded by the gray area is the reconstruction by *Svalgaard and Cliver* [2010] (SC10), the gray area being the uncertainty range computed in the present paper. Solid circles show annual means of IMF observations.

the present day. After 1960 more than 40 stations are used, whereas before 1880 there is just one available.

[13] REA07 used two combinations of the corrected *aa* index, aa_C; one with the median *m* index (compiled from hourly means from a number of observatories) the other with an earlier version of the IDV index by *Svalgaard and Cliver* [2005]. Because of potential inhomogenities in the hourly data before 1895 (particularly the prevalence of hourly "spot" samples rather than full hourly means), REA07 limited their reconstruction to after 1895. The *aa* and aa_C indices are "range" indices because they are based on the range of variation in 3 h intervals, derived from two data sequences (one from southern England, one from Australia: in both cases the series is a composite from 3 stations). The *aa* index has been corrected to aa_C by correlation with other range indices, from a greater number of stations, such as Ap and Am. This correction found and removed a skip in calibration caused by the move of the northern hemisphere *aa* station from Abinger to Hartland. In addition, a slow drift in calibration in recent years was detected and corrected for. As for IDV, the *m* index was based on a number of stations which increased from 1 to 36 over the interval covered. However, unlike the daily IDV values, each station was used to generate 24 separate data series (one for each UT) and the number of station UTs ranged from 24 to over 400. The REA07 method was based on the finding that aa_C, *m* and IDV correlated best with various combinations of *B* and *V* and that the differences were statistically significant. In addition to using different combinations of indices, REA07 used two different regression fitting procedures. The plot shown in Figure 1 is for the aa_C and *m* indices using a Bayesian least squares method, but results for ordinary least squares fits were generally very similar (see REA07, Figure 5).

[14] LEA09 used the combination of the corrected aa index, aa_C, and the median index *m*, with ordinary least squares regression. This reconstruction was extended back to only 1905 because the results of REA07 showed some dependence on regression procedure before this date: consequently, LEA09 set a higher threshold number of stations required to be contributing to the m index and their reconstruction only extends back to 1905.

[15] As described above, the LEA99 curve presented here is a polynomial fit of equation (2) to the corrected aa index, aa_C, which is available for 1868 to the present day. Despite this wide range of data types, data sources and reconstruction methods, the results in Figure 1 are remarkably similar. Values from the LEA99 method are generally slightly lower than the SC10 variation before about 1960. The REA07 reconstruction shows a very low value in 1901; however, the value for this particular year did vary somewhat with the data/method combinations studied by REA07 and is anomalous as this is the only year for which there is any significant difference to SC10. As noted by SC10, LEA09 is only significantly different in solar cycle 14 (1901–1912), when it gives slightly lower values.

4. Uncertainty Analysis of the Variation of SC10

[16] Because the method of SC10 is relatively straightforward (making use of a single correlation), it has the advantage that it is much easier to study the propagation of uncertainties than when a combination of two indices are used, as in REA07 and LEA09. In addition, the authors give the uncertainties in the linear regression coefficients that they derived. Their reconstruction of *B* is the average of two fits, so the functional form for *B* in terms of the IDV index, I_{DV}, used is:

$$B = 0.5\left(a + b\ I_{DV} + c\ I_{DV}^{\ p}\right) \tag{4}$$

and the best fit coefficients they derive are $a \pm \Delta a = 2.06 \pm 0.21$, $b \pm \Delta b = 0.4421 \pm 0.021$, $c \pm \Delta c = 1.33 \pm 0.07$ and $p \pm \Delta p = 0.689 \pm 0.21$. Propagating the uncertainties through equation (4) using the partial derivatives for all the variables, x, in equation (4)

$$\Delta B_{IDV}^2 = \sum\nolimits_x |\partial B_{IDV}/\partial x|^2 \Delta x^2 \tag{5}$$

yields

$$\Delta B_{IDV}^2 = 0.25\Big\{\Delta a^2 + I_{DV}^2\ \Delta b^2 + I_{DV}^{2p}\left(\Delta c^2 + c^2(\log_e I_{DV})^2 \Delta p^2\right) + \left(b + cpI_{DV}^{p-1}\right)\Delta I_{DV}^2\Big\} \tag{6}$$

For ΔI_{DV} we here use the standard error in the mean $= \sigma/(N)^{1/2}$ where σ is the population standard deviation and *N* is the number of stations contributing to IDV. We use $\sigma = 1.25$nT, based on the spread of IDV values for individual stations for the modern era when *N* is large. Note that we assume that σ has remained constant. This will almost certainly underestimate the uncertainties in the earlier years because instrument accuracy was probably lower then, which would make σ greater than it has been in modern times. In other words, the error analysis allows for the regression uncertainties and the statistical effects of sampling with a limited number of observatories, but cannot account for any drifts in instrument calibration. This unknown source of error may be particularly important early in the series when *N* is small and magnetometer instrumentation and methods were still developing. The gray area in Figure 1 is bounded by $(B_{IDV} - \Delta B_{IDV})$ and $(B_{IDV} + \Delta B_{IDV})$. It can be seen uncertainties are low, even at the start of the sequence when $N = 1$. As noted by SC10, the worst disagreement between the reconstructions occurs for the solar minima between 1870 and 1920 which is when average *B* values derived from cosmogenic isotopes by *Steinhilber et al.* [2010, hereafter SEA10] are also lower. This comparison is discussed further in section 6.

5. Open Solar Flux F_S Reconstructions

[17] Figure 2 shows various reconstructions of open solar flux F_S, using the same color scheme as Figure 1. The variations LEA99, REA07 and LEA09 are as they appear in the original papers whereas SC10 has been estimated from the variation in *B* that they present. To make the conversion from SC10 *B* estimates to F_S, we here adopt the preaveraging interval of $t = 1$ day, which was also used by REA. Figure 3 shows the scatterplot of observed annual means ($T = 1$ year) of $\langle |B_r|_t \rangle_T$ against $\langle B \rangle_T$ for $t = 1$ day. This is the same plot as presented by *Lockwood et al.* [2006], but here updated to cover 1963–2009, inclusive, and so include data from the recent solar minimum. The solid line shows the ordinary least

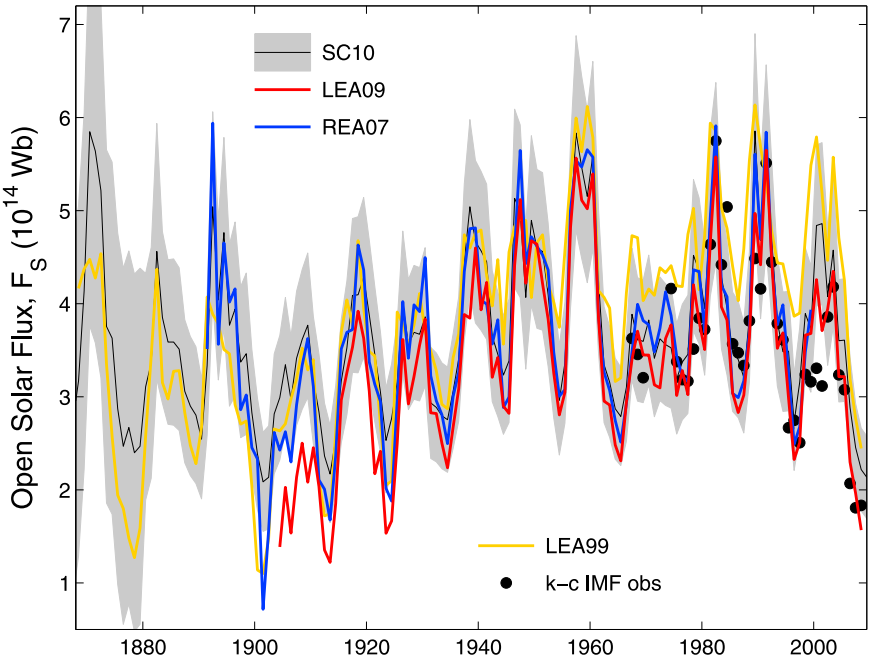

Figure 2. Reconstructions of the open solar flux, F_S, from geomagnetic activity data. The color scheme is the same as in Figure 1. The variations are as they appear in the publications except that attributed to *Svalgaard and Cliver* [2010] (SC10), which is their variation in B converted to F_S using equations (1) and (7). The solid circles are the values derived from interplanetary observations using the kinematic correction described by *Lockwood et al.* [2009b].

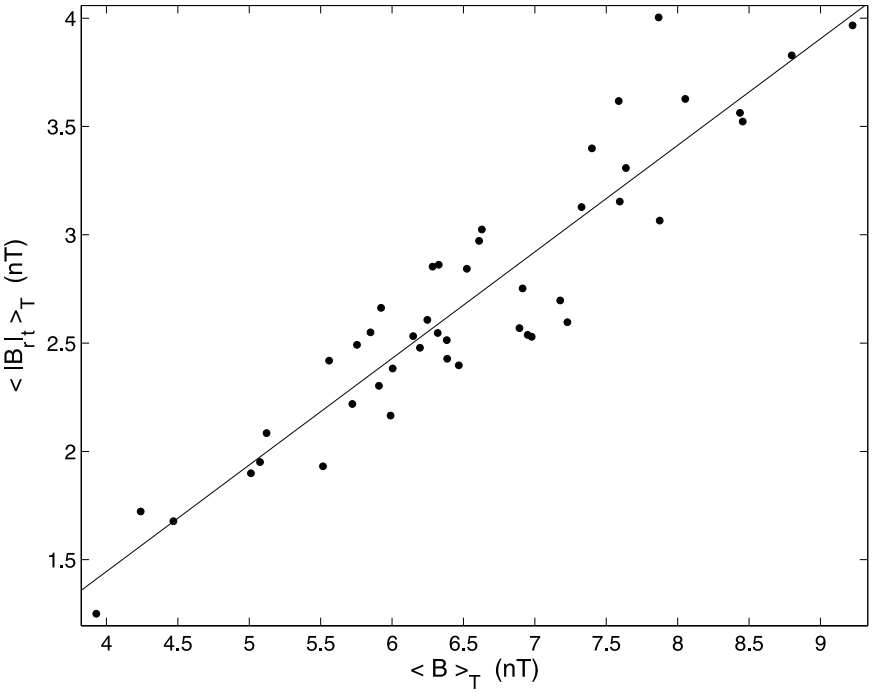

Figure 3. Scatterplot of the mean of the modulus of the radial IMF, $\langle |B_r|_t \rangle_T$ as a function of IMF magnitude $\langle B \rangle_T$ for the OMNI2 data set for 1963–2010. The preaveraging timescale (on which the modulus is taken) is $t = 1$ day, and the final averaging timescale is $T = 1$ year. Only means for years with >25% data availability are included in the plot and the regression. The correlation coefficient is $r = 0.93$ (significance level 99.88%), and the ordinary best fit linear regression fit shown has a slope $d = 0.492 \pm 0.029$ and an intercept $e = -0.522 \pm 0.136$.

squares best regression fit (for errors in both variables) given by

$$\langle |B_r|_t \rangle_T = (d \pm \Delta d)\langle B \rangle_T + (e + \Delta e) = (0.492 + 0.029)\langle B \rangle_T - (0.522 \pm 0.136) \quad (7)$$

Note that this linear regression cannot apply at very small fields because $\langle B \rangle_T$ below about 1nT would yield negative $\langle |B_r|_t \rangle_T$. However, the departure from the linear form cannot be detected even in the lowest $\langle B \rangle_T$ values in Figure 3. The open flux F_S is computed from $\langle |B_r|_t \rangle_T$ using equation (1). The uncertainty ΔF_S is computed by the equivalent of equation (6), including the additional uncertainties Δd and Δe. The solid circles in Figure 2 are the values derived from interplanetary observations using the kinematic correction to allow for the excess flux effect at r = 1AU, as described by *Lockwood et al.* [2009b].

[18] LEA09 reviewed the differences between the derived F_S reconstructions and Figure 2 adds the implications of the SC10 reconstruction of B to this comparison. As for the IMF B (Figure 1), the reconstructions of F_S are remarkably similar. Uncertainties in the SC10 variation are larger than in Figure 1 because of the need to use equation (7) to convert B into F_S. Because the SC10 and REA07 variations both use t = 1 day they are directly comparable and do agree very closely indeed (with the notable exception of the 1901 data point). The LEA99 variation is that which appeared in the original paper and was derived using t = 1 h, hence it does not allow for the kinematic effect and is consistently greater that the kinematically corrected IMF observations. At earlier times, the effect of the 1957 calibration discontinuity in *aa* at least partially offsets the effect of using t = 1hr. The LEA09 reconstruction is the only one to make use of the kinematic correction (quantified for historic geomagnetic data using the recurrence of the aa_C index) and this does make a significant difference, giving lower values at the start of the series, particularly in solar cycle 14 (1901–1912). Evidence in support of this comes from the recent solar minimum (2008–2010) when F_S fell to similar values as the reconstructed values at the start and end of cycle 14: in this minimum, the LEA09 reconstruction matches the kinematically corrected values from IMF data better than the other reconstructions.

6. The Floor Value of *B*

[19] *Svalgaard and Cliver* [2007, hereafter SC07] postulated that annual means of the near-Earth heliospheric field B could not fall below a floor value 4.6nT. Because observed values have fallen below this level during the recent solar minimum, SC10 have revised this estimate to 4 nT. One aspect in which the reconstructions in Figure 1 do differ relates to their implications for any floor in annual mean B values. In this section, we use the terminology that the floor value is the minimum of B below which it cannot fall even on millennial timescales. We make the distinction between such a floor value and the minimum seen in any one data or reconstruction time series which cover a more limited interval.

[20] The existence, or otherwise, of a floor in the IMF strength will ultimately be determined by the relative magnitudes of open solar flux production and loss rates [*Solanki et al.*, 2000; *Vieira and Solanki*, 2010] and their variations with solar activity levels. The floor value would be at the solar activity level below which the loss rate for open flux becomes smaller than its production rate, so that further loss is not possible. Loss of open solar flux over recent solar cycles has been shown to be related to the inclination of the heliospheric current sheet, HCS [*Owens et al.*, 2011] a possibility raised by the study by *Sheeley and Wang* [2001] of inferred near-Sun reconnection points. Thus a floor in open solar flux would be associated with a very flat HCS. Observations from the last three solar minima show that the HCS has maintained a higher level of inclination with decreasing open solar flux [e.g., *Owens et al.*, 2011]. From PFSS modeling, *Wang et al.* [2009] suggest that the high inclination of the HCS during periods of weak polar field periods is probably associated with the inability of the polar fields to close down (through reconnection) emerging nonaxisymmetric magnetic fields. This implies that as the level of solar activity decreases, the open solar flux loss rate does not decrease more rapidly than the open flux emergence rate, in which case no floor value would be reached. Furthermore, the continued cycling of ^{10}Be throughout Maunder Minimum [*Beer et al.*, 1998] could be due to continued, if low, production and loss of open solar flux even at extremely low open solar flux levels. If this were the case, it would mean that the loss rates, at least during parts of the cycle, exceeded the production rate even at very low levels of activity. However, other explanations are possible: the cosmic rays that generate ^{10}Be are scattered by irregularities in the heliospheric field (rather than the field itself) and are subject to gradient and curvature drifts and hence the cyclic behavior of ^{10}Be may not relate to matching oscillations in open solar flux (if a mechanism were to be active whereby the irregularity density was cyclically enhanced for a constant low level of open solar flux, for example the cyclic appearance of CIRs covering a large latitude range or of CMEs).

[21] Figure 4 (top) shows the full data sequence of SC10 from 1835 onward. The black line is B_{IDV}, and the gray area gives the uncertainties $\pm\Delta B_{IDV}$ computed here. The floor values proposed by SC07 and SC10 are shown by horizontal dashed lines labeled SC10 and SC07. The lowest value in the SC10 reconstruction of B_{IDV} is 4.06 nT, set in 1901, but allowing for the uncertainty, ΔB_{IDV} the lowest value of ($B_{IDV} - \Delta B_{IDV}$) is 3.52 nT, set in 1855. (Note that the 1901 value of ($B_{IDV} - \Delta B_{IDV}$) is 3.71 nT.) The minimum of the REA07 reconstruction shown is 2.08 nT, again set in 1901. However, this value is notably lower than others around it in the REA07 reconstruction, and it is not matched by all of the analysis combinations discussed by REA07. The 1901 value of 2.08 nT was found using the m and aa_C indices with the Bayesian least squares regression technique, the same combination of indices using the ordinary least squares method yielding 2.93 nT. Hence this low value appears to be a feature of the m index which in 1901 is based on only the Potsdam data series. Using IDV [from *Svalgaard and Cliver*, 2005] and aa_C, REA07 find minima of 3.40 nT and 4.50 nT using Bayesian and ordinary least squares fits, respectively (both set in 1901), compared to the SC10 value for 1901 of $B_{IDV} \pm \Delta B_{IDV}$ 4.05 ± 0.35. This demonstrates the influence of the regression procedure used as well as that of the data employed [*Lockwood et al.*, 2006]. The minimum of the variation derived here using the LEA99 method is 2.37 nT, again set

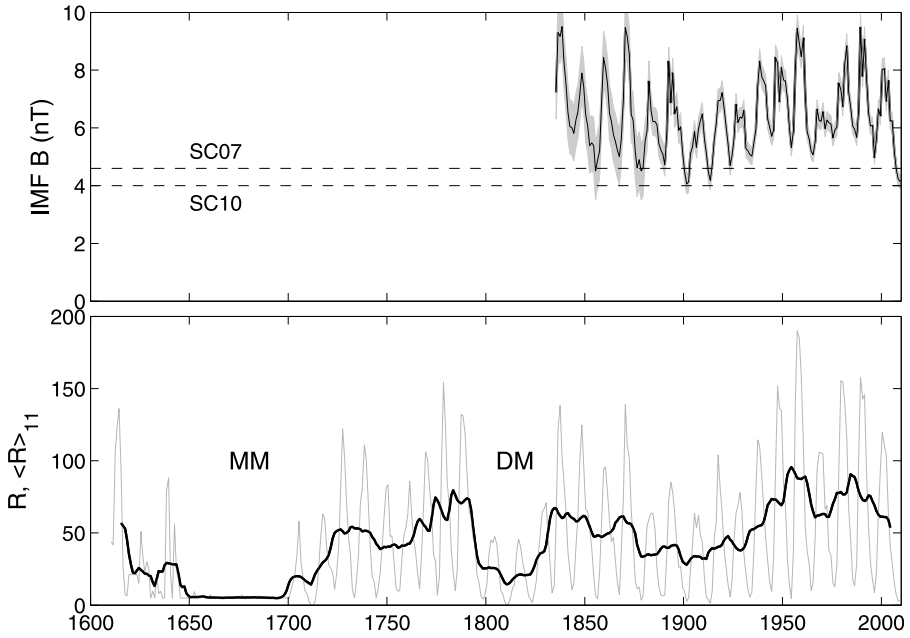

Figure 4. (top) The SC10 variation in heliospheric field B derived from geomagnetic activity. The black line shows the value derived by *Svalgaard and Cliver* [2010], and the gray area is the uncertainty range evaluated here. Also shown as horizontal dashed lines are the floor estimates of *Svalgaard and Cliver* [2007] and *Svalgaard and Cliver* [2010] (labeled SC07 and SC10, respectively). (bottom) The sunspot number record. Data after 1700 are the international sunspot numbers [*SIDC-team*, 2010] whereas before this date, linearly regressed group sunspot numbers are used. The gray line shows annual means and the black line the 11 year running means. The Maunder and Dalton minima are labeled MM and DM, respectively.

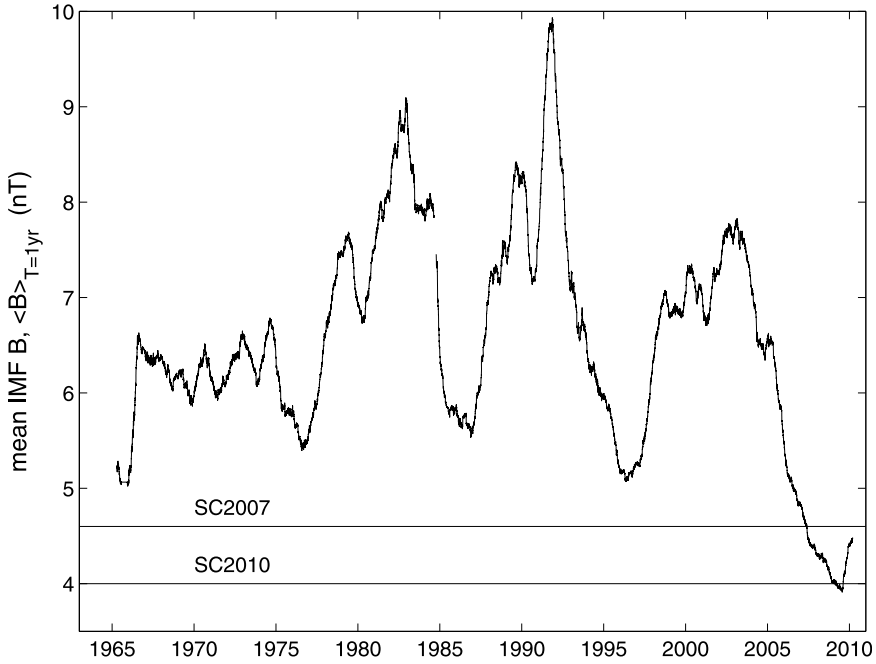

Figure 5. The variation of daily running means of the IMF field strength $\langle B \rangle_T$ from near-Earth spacecraft for an averaging interval of T = 1 year. Also shown are the floor estimates of SC07 and SC10, as in Figure 4 (top).

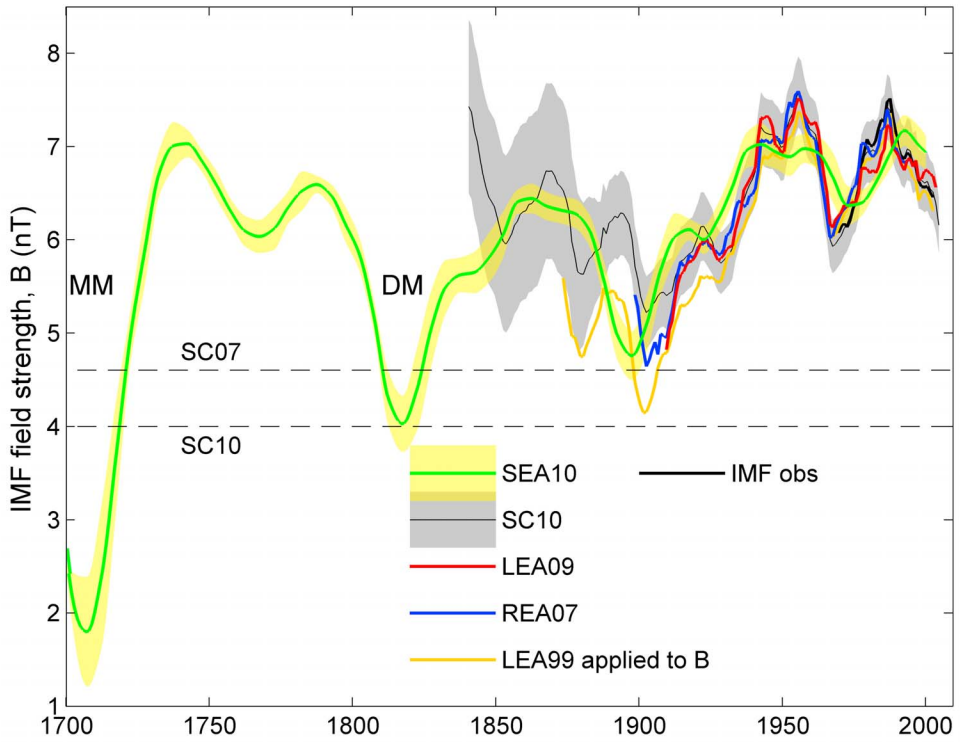

Figure 6. Eleven year running means of the reconstructions of B shown in Figure 1, plotted using the same color scheme. The green line shows the 25 year running means of B deduced from cosmogenic isotope abundances by *Steinhilber et al.* [2010] (SEA10), and the surrounding yellow band is their estimate of the uncertainty. The (end of) the Maunder minimum and the Dalton minimum are labeled MM and DM, respectively. The floor estimates of *Svalgaard and Cliver* [2010] (SC10) and *Svalgaard and Cliver* [2010] (SC07) are for annual mean data and so should be lower than the 11 and 25 year means presented.

in 1901. The lowest value in the LEA09 reconstruction is 4.0 nT, set in 2009. However, it should be noted that LEA09 placed a more stringent threshold on the required number of station UTs contributing to the m index than did REA07 and so did not predict a value for 1901.

[22] In fact, a lower limit is set by direct observations of the IMF than some of the reconstructed values listed above. Figure 5 shows that during the recent minimum, annual means of the observed IMF B fell to 3.9 nT. This plot shows daily running means of B averaged over 365 days (which will generally fall to lower values than the averages taken over calendar years, depending on the precise timing of the minimum in B within the calendar year). The minimum in $\langle B \rangle_{T\,=\,1yr}$ between cycles 19 and 20 may not be fully defined but appears to be 5.02 nT and the subsequent minima are 5.40 nT, 5.54 nT, 5.07 nT and 3.91 nT. Hence the observations during the recent minimum shows that the minimum B can fall by 23% over just one solar cycle, stressing its considerable variability.

[23] The differences between the reconstructions in Figure 1 occur early in the sequences when geomagnetic data were sparse and almost certainly less reliable. Interestingly, the worst disagreements occur for the solar minima between 1870 and 1920 which, as noted by SC10, is when average B values derived from cosmogenic isotopes by SEA10 are also lower. However, it is not here argued that any one reconstruction is better than another, just that the uncertainties inherent in the reconstructions make identification of the minimum value, let alone a floor, very difficult. Note that it is not just the recently observed minimum that calls for the downward revision of the floor: B from the SC10 reconstruction for the years 1855, 1878, 1900, 1901, 1902, 1912, 1913, 2007, 2008 and 2009 are all below the SC07 floor estimate. Allowing for the uncertainties, the minimum of the annual values of $(B_{IDV} - \Delta B_{IDV})$ is 3.5 nT and, given that the IMF observations show that annual means can fall to 3.9 nT, the best estimate of the minimum value since 1835 could be considered to be 3.7 ± 0.2nT.

[24] It is a separate question as to if these minima define a genuine floor in B. The present authors argue that demonstration of a floor would require repeated minima in B close to a level below which it never falls. There are two approaches to the SC10 floor value in Figure 4 (top), the first around 1900 and the second in the recent solar minimum. However, until we observe the next solar minimum we cannot be sure that the long-term decline to the recent minimum has ended [*Lockwood*, 2010] and so the geomagnetic data show just one, potentially two, approaches to this minimum. Two such events could easily occur by chance. Figure 4 (bottom) shows the sunspot number record (as both annual means and 11 year running means). Data after 1700 are the international sunspot numbers [*SIDC-team*, 2010] whereas before this date linearly regressed group sunspot numbers are used. The value of B = 3.7 ± 0.2nT is the estimated lowest value that has existed

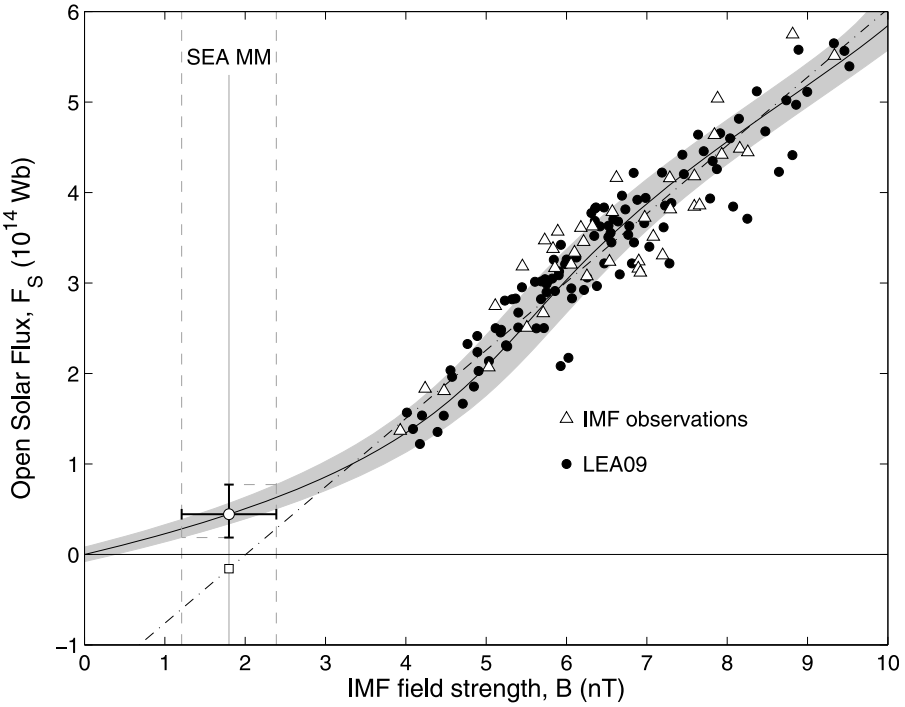

Figure 7. Scatterplot of open solar flux, F_S, kinematically corrected to allow for the excess flux effect, as a function of field strength B. The solid points are the reconstruction of *Lockwood et al.* [2009a] (the LEA09 plots in Figures 1 and 2), and the open triangles are annual means from IMF observations. The dot-dash line is an ordinary least squares linear regression fit, the black line is a polynomial fit constrained to pass through the origin ($F_S = 0$, $B = 0$) and given by equation (8) in text, and the surrounding gray area shows the uncertainty in that polynomial fit at the 2σ level. The vertical dashed lines are the limits of the estimate by *Steinhilber et al.* [2010] of B at the end of the Maunder minimum (the best estimate is the vertical solid line marked SEA MM and is 1.80 ± 0.59 nT). The analysis in the present paper yields a best estimate for F_S at this time of $(0.48 \pm 0.29) \times 10^{14}$ Wb.

during the interval of geomagnetic data that have been used thus far (i.e., 1835 onward). But Figure 4 shows that these data do not extend back into the Dalton sunspot minimum (labeled DM in Figure 4), let alone the Maunder minimum (MM) and the earlier, even deeper (and longer-lasting) grand solar minima seen in the cosmogenic isotope records [e.g., *Steinhilber et al.*, 2008].

[25] To investigate this further, Figure 6 compares 11 year running means of the IMF reconstructions from geomagnetic activity shown in Figure 1 with 25 year running means of the estimates of B made by SEA10 using cosmogenic isotope data and a simple theory of cosmic ray shielding (labeled SEA10 in Figure 6). The plot shown is their reconstruction which allows for a solar wind speed variation and is based on the 25 year running mean of the φ_{PCA}, the heliospheric modulation parameter derived by *Steinhilber et al.* [2008] from ^{10}Be cosmogenic isotope abundances and neutron monitor data. The area shaded yellow is their estimate of the uncertainty. SEA10 show that this variation has many similarities to other estimates of the heliospheric field variation derived from cosmogenic isotopes; consequently they are not reviewed here. The agreement with the results from geomagnetic activity is again remarkably good, considering that the derivation and data source is completely independent. The 25 year means of the SEA10 reconstruction fall to the proposed SC10 floor value of 4 nT during the Dalton minimum (so annual means at the minima of the sunspot cycles will be lower than this) and even the 25 year means fall to 1.80 ± 0.59 nT by the end of the Maunder minimum. Extending the sequence over 9300 years, SEA10 find 14 grand solar minima in which the reconstructed B fell to even lower values in 25 year means. Given the good agreement with the reconstructions based on geomagnetic activity during the period of overlapping data (as shown by Figure 6), this is very strong evidence that if a floor in IMF B values does exist, it is much smaller than the lowest values seen during recent centuries.

[26] Subsequent to submitting the present paper, *Cliver and Ling* [2010] have generated a new estimate of the floor IMF value of B about 2.8nT (in yearly means). This further downward revision was achieved using two correlations; the first between solar polar-field strength and yearly averages of B for the last four solar cycle minima the second between peak sunspot number for cycles 14–23 and B at the preceding minima. This is a much sounder argument than the lowest value seen in a given data series. However, Cliver and Ling correctly note that these relationships are assumed to be linear when extrapolated right down to Maunder minimum conditions. In this context we note that the first correlation is only for data taken within a grand solar maximum and the second has considerable scatter which certainly makes the assumed

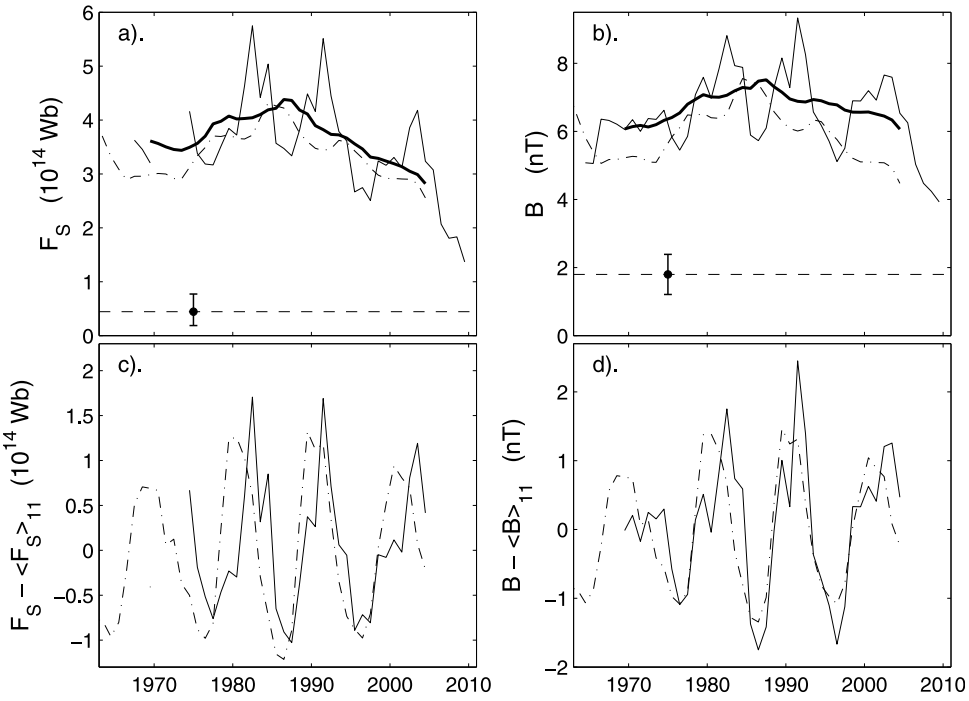

Figure 8. Variations detected by interplanetary spacecraft of (a and c) open solar flux, F_S, and (b and d) near-Earth IMF, B. Figures 8a and 8b show observed annual means as thin lines and 11 year running means as thick lines; Figures 8c and 8d show the solar cycle variations by plotting the deviation of the annual means from the 11 year running mean to remove the drift. In Figures 8a and 8b the horizontal dashed line gives, respectively, the value estimated in the present paper and by *Steinhilber et al.* [2010] (SEA10) for the end of the Maunder minimum, with the computed uncertainty given by the error bar. The dot-dash line shows the scaled variations of sunspot number: Figures 8a and 8b show $\langle R \rangle_{11}/S$ and Figures 8c and 8d show $(R - \langle R \rangle_{11})$/S where the scaling factors S (to give the y scale values shown) are 21, 12, 62 and 56 for Figures 8a–8d, respectively.

linear relationship questionable and would give a very large uncertainty in the minimum B even for a linear fit.

7. The Open Solar Flux at the End of the Maunder Minimum

[27] Figure 7 is an updated and annotated version of Figure 12 of LEA09. It shows a scatterplot of annual means of open solar flux F_S as a function of the corresponding near-Earth IMF B values. The open solar flux values employ the correction developed by *Lockwood et al.* [2009b] to allow for the kinematic "excess flux" effect between the coronal source surface and the spacecraft. The black dots are from the LEA09 reconstruction for 1905–2009, the open triangles are observations from near-Earth interplanetary craft. The dashed line is a linear regression fit to all data points; if this linear relation applied then IMF B would reach a floor near 2nT when the open solar flux fell to zero. However, this makes no sense physically as the open solar flux is the source of the field in the heliosphere. Thus a more realistic polynomial fit, constrained so that $B = 0$ when $F_S = 0$, has been made. With such a constraint, the best polynomial fit (to both the reconstruction from geomagnetic data and the interplanetary observations) is the black line, given by

$$B_{\rm fit} = 4.7386\ F_S - 1.7202\ F_S^2 + 0.3329\ F_S^3 - 0.0218\ F_S^4 \quad (8)$$

The gray area bounds the 2σ uncertainty in the fit.

[28] Using the SEA10 estimate that the near-Earth IMF B fell to 1.80 ± 0.59 nT by the end of the Maunder minimum, Figure 7 shows that the fitted polynomial yields an estimate of the open solar flux of (0.48 ± 0.29) × 10^{14} Wb at this time. This is slightly lower than the estimate of (1.01 ± 0.49) × 10^{14} Wb obtained by SEA10. The difference arises mainly from the different methods used to convert from B to B_r: *Steinhilber et al.* [2010] used the linear regression of *Lockwood et al.* [2006] (updated here in Figure 3) in which an averaging interval of t = 1 day was employed. On the other hand, Figure 7, and the F_S value scaled from it, uses the kinematic correction, as implemented by *Lockwood et al.* [2009b].

[29] The modeling of *Solanki et al.* [2000] and *Vieira and Solanki* [2010] used an initial starting condition that the open solar flux at the end of the Maunder minimum was zero. The nonzero value reported here would only influence of their modeled values very early in the sequence as the effect of the initial condition is soon lost as the modeling advances in time. *Lockwood* [2003] used the model of *Solanki et al.* [2000], but ran it backward in time from an initial starting condition which was the open solar flux deduced during the first perihelion pass of the Ulysses spacecraft in 1994–5: the value of F_S derived for the end of the Maunder minimum was 1 × 10^{14} Wb which is the same as obtained from cosmogenic isotopes by SEA10 but slightly larger than the estimate obtained here. However, like SEA10, *Lockwood* [2003]

employed $t = 1$ day and so the lower value is again due to the allowance for the kinematic excess flux effect of longitudinal solar wind flow variations.

8. Conclusions

[30] This paper has shown that the predictions of open solar flux by *Lockwood et al.* [1999] (LEA99) were consistent with the growing consensus on how the IMF has varied over the past 150 years. Disagreements between reconstructions of B do occur early in the sequences where the geomagnetic data were sparse and less reliable. Therefore any minimum values in B are very hard to define, and insufficient to establish the existence of a floor.

[31] The estimate by *Steinhilber et al.* [2010] (SEA10), made using cosmogenic isotopes, that the near-Earth IMF B fell to 1.80 ± 0.59 nT by the end of the Maunder minimum is consistent with an open solar flux of $0.48 \pm 0.29 \times 10^{14}$ Wb at this time.

[32] Figure 8 places the derived values for the end of the Maunder minimum in context with the modern observations of interplanetary space. Figures 8a and 8b show the annual means (thin line) and the 11 year running means (thick line), Figure 8a shows F_S and $\langle F_S \rangle_{11}$, and Figure 8b shows B and $\langle B \rangle_{11}$. Also shown (as a dot-dash line) is the equivalent variation of the 11 year running means of the sunspot number $\langle R \rangle_{11}/S$, where S is an arbitrary scaling factor. The values for the end of the Maunder minimum are shown as a horizontal dashed line (with the estimated uncertainty given by the error bar): for F_S (Figure 8a) this is the value derived in the present paper and for B (Figure 8b) this is the value derived by *Steinhilber et al.* [2010]. Figures 8c and 8d show the corresponding detrended solar cycle variations; $(F_S - \langle F_S \rangle_{11})$ in Figure 8c and $(B - \langle B \rangle_{11})$ in Figure 8d, along with a dot-dash line showing the corresponding scaled variation for sunspot number $(R - \langle R \rangle_{11})/S$. It can be seen that the recent decline in $\langle F_S \rangle_{11}$ is consistent with that in $\langle R \rangle_{11}$ and, given that sunspot number falls to near zero in the Maunder minimum, this is consistent with the fall to very low open solar flux in the Maunder minimum. Thus $\langle F_S \rangle_{11}$ appears to be closely related to $\langle R \rangle_{11}$. Figure 8b shows that the decline in $\langle B \rangle_{11}$ has not been as rapid as that in $\langle R \rangle_{11}$. Figures 8c and 8d show the solar cycle variations, after the trends have been removed and both B and F_S peak roughly 2 years after sunspot maximum. A similar lag is seen in the 11 year smoothed variations in Figures 8a and 8b. This implies that the emergence and loss processes that determine the continuity equation of F_S are the same for the centennial scale drift as for the solar cycle. This offers the possibility that the HCS plays the same role on centennial timescales as defined for the solar cycle by *Owens et al.* [2011]. The peak around 1985 in $\langle F_S \rangle_{11}$, $\langle B \rangle_{11}$ and $\langle R \rangle_{11}$ appears increasingly to be a grand solar maximum [*Lockwood and Fröhlich*, 2007; *Lockwood et al.*, 2009a; *Steinhilber et al.*, 2008; *Abreu et al.*, 2008]. From Figure 8a we see that this peak (of $\langle F_S \rangle_{11} = 4.382 \times 10^{14}$ Wb) is greater than at the end of the Maunder minimum by $(3.94 \pm 0.29) \times 10^{14}$ Wb. From Figure 8c we can deduce that the typical amplitude (minimum to maximum) of open solar flux over recent solar cycles has been about 2.5×10^{14} Wb, from which we deduce that the long-term drift in F_S from the Maunder minimum to the recent grand maximum is about 50% larger than recent solar cycle amplitudes and that mean levels of the open solar flux during the Maunder minimum were about 11% of the mean values at the peak of the recent grand solar maximum.

[33] **Acknowledgments.** The authors are grateful to the many scientists who contributed to the compilation of the geomagnetic and interplanetary data shown here. The Omni2 interplanetary data were obtained from the Space Physics Data Facility at NASA's Goddard Space flight center. The international sunspot numbers were obtained from the World Data Center for the Sunspot Index, and the group sunspot numbers were obtained from NOAA's National Geophysical data center. They also thank L. Svalgaard for valuable discussions.

[34] Philippa Browning thanks the reviewers for their assistance in evaluating this paper.

References

Abreu, J. A., et al. (2008), For how long will the current grand maximum of solar activity persist?, *Geophys. Res. Lett.*, *35*, L20109, doi:10.1029/2008GL035442.

Beer, J., S. Tobias, and N. Weiss (1998), An active Sun throughout the Maunder Minimum, *Sol. Phys.*, *181*, 237–249, doi:10.1023/A:1005026001784.

Cliver, E. W., and A. G. Ling (2010), The floor in the solar wind magnetic field revisited, *Sol. Phys.*, doi:10.1007/s11207-010-9657-6.

Finch, I. D., and M. Lockwood (2007), Solar wind-magnetosphere coupling functions on timescales of 1 day to 1 year, *Ann. Geophys.*, *25*, 495–506, doi:10.5194/angeo-25-495-2007.

Jones, G. H., A. Balogh, and R. J. Forsyth (1998), Radial heliospheric magnetic fields detected by Ulysses, *Geophys. Res. Lett.*, *25*, 3109–3112, doi:10.1029/98GL52259.

Lagarias, J. C., J. A. Reeds, M. H. Wright, and P. E. Wright (1998), Convergence properties of the Nelder–Mead simplex method in low dimensions, *J. Opt.*, *9*(1), 112–147, doi:10.1137/S1052623496303470.

Lockwood, M. (2003), Twenty-three cycles of changing open solar magnetic flux, *J. Geophys. Res.*, *108*(A3), 1128, doi:10.1029/2002JA009431.

Lockwood, M. (2010), Solar change and climate: An update in the light of the current exceptional solar minimum, *Proc. R. Soc. A*, *466*, 303–329, doi:10.1098/rspa.2009.0519.

Lockwood, M., and C. Fröhlich (2007), Recent oppositely directed trends in solar climate forcings and the global mean surface air temperature, *Proc. R. Soc. A*, *463*, 2447–2460, doi:10.1098/rspa.2007.1880.

Lockwood, M., and M. J. Owens (2009), The accuracy of using the Ulysses result of the spatial invariance of the radial heliospheric field to compute the open solar flux, *Astrophys. J.*, *701*(2), 964–973, doi:10.1088/0004-637X/701/2/964.

Lockwood, M., R. Stamper, and M. N. Wild (1999), A doubling of the Sun's coronal magnetic field during the past 100 years, *Nature*, *399*, 437–439, doi:10.1038/20867.

Lockwood, M., R. B. Forsyth, A. Balogh, and D. J. McComas (2004), Open solar flux estimates from near-Earth measurements of the interplanetary magnetic field: Comparison of the first two perihelion passes of the Ulysses spacecraft, *Ann. Geophys.*, *22*, 1395–1405, doi:10.5194/angeo-22-1395-2004.

Lockwood, M., A. P. Rouillard, I. Finch, and R. Stamper (2006), Comment on "The IDV index: Its derivation and use in inferring long-term variations of the interplanetary magnetic field strength" by Leif Svalgaard and Edward W. Cliver, *J. Geophys. Res.*, *111*, A09109, doi:10.1029/2006JA011640.

Lockwood, M., A. P. Rouillard, and I. D. Finch (2009a), The rise and fall of open solar flux during the current grand solar maximum, *Astrophys. J.*, *700*, 937–944, doi:10.1088/0004-637X/700/2/937.

Lockwood, M., M. Owens, and A. P. Rouillard (2009b), Excess open solar magnetic flux from satellite data: 2. A survey of kinematic effects, *J. Geophys. Res.*, *114*, A11104, doi:10.1029/2009JA014450.

Nelder, J. A., and R. Mead (1965), A simplex method for function minimization, *Comput. J.*, *7*, 308–313.

Owens, M. J., C. N. Arge, N. U. Crooker, N. A. Schwadron, and T. S. Horbury (2008), Estimating total heliospheric magnetic flux from single-point in situ measurements, *J. Geophys. Res.*, *113*, A12103, doi:10.1029/2008JA013677.

Owens, M. J., N. U. Crooker, and M. Lockwood (2011), How is open solar magnetic flux lost over the solar cycle?, *J. Geophys. Res.*, doi:10.1029/2010JA016039, in press.

Riley, P., and J. T. Gosling (2007), On the origin of near-radial magnetic fields in the heliosphere: Numerical simulations, *J. Geophys. Res.*, *112*, A06115, doi:10.1029/2006JA012210.

Rouillard, A. P., M. Lockwood, and I. Finch (2007), Centennial changes in the solar wind speed and in the open solar flux, *J. Geophys. Res.*, *112*, A05103, doi:10.1029/2006JA012130.

Sheeley, N. R., Jr., and Y.-M. Wang (2001), Coronal inflows and sector magnetism, *Astrophys. J.*, *562*, L107–L110, doi:10.1086/338104.

SIDC-team (2010), Monthly report on the international sunspot mumber, online catalogue of the sunspot index, World Data Cent. for the Sunspot Index R. Obs. of Belgium,, Brussels. [Available at http://www.sidc.be/sunspot-data/.]

Solanki, S. K., M. Schüssler, and M. Fligge (2000), Evolution of the Sun's large-scale magnetic field since the Maunder minimum, *Nature*, *408*, 445–447, doi:10.1038/35044027.

Stamper, R., M. Lockwood, M. N. Wild, and T. D. G. Clark (1999), Solar causes of the long term increase in geomagnetic activity, *J. Geophys. Res.*, *104*, 28,325–28,342, doi:10.1029/1999JA900311.

Steinhilber, F., J. A. Abreu, and J. Beer (2008), Solar modulation during the Holocene, *Astrophys. Space Sci. Trans.*, *4*, 1–6, doi:10.5194/astra-4-1-2008.

Steinhilber, F., J. A. Abreu, J. Beer, and K. G. McCracken (2010), Interplanetary magnetic field during the past 9300 years inferred from cosmogenic radionuclides, *J. Geophys. Res.*, *115*, A01104, doi:10.1029/2009JA014193.

Svalgaard, L., and E. W. Cliver (2005), The IDV index: Its derivation and use in inferring long-term variations of the interplanetary magnetic field strength, *J. Geophys. Res.*, *110*, A12103, doi:10.1029/2005JA011203.

Svalgaard, L., and E. W. Cliver (2007), Interhourly variability index of geomagnetic activity and its use in deriving the long-term variation of solar wind speed, *J. Geophys. Res.*, *112*, A10111, doi:10.1029/2007JA012437.

Svalgaard, L., and E. W. Cliver (2010), Heliospheric magnetic field 1835–2009, *J. Geophys. Res.*, *115*, A09111, doi:10.1029/2009JA015069.

Vieira, L. E. A., and S. K. Solanki (2010), Evolution of the solar magnetic flux on time scales of years to millennia, *Astron. Astrophys.*, *509*, doi:10.1051/0004-6361/200913276.

Wang, Y.-M., and N. R. Sheeley Jr. (1995), Solar implications of Ulysses interplanetary field measurements, *Astrophys. J.*, *447*, L143–L146.

Wang, Y.-M., E. Robbrecht, and N. R. Sheeley (2009), On the weakening of the polar magnetic fields during solar cycle 23, *Astrophys. J.*, *707*, 1372–1386, doi:10.1088/0004-637X/707/2/1372.

Yeates, A. R., D. H. Mackay, A. A. van Ballegooijen, and J. A. Constable (2010), A nonpotential model for the Sun's open magnetic flux, *J. Geophys. Res.*, *115*, A09112, doi:10.1029/2010JA015611.

M. Lockwood and M. J. Owens, Space Environment Physics Group, Department of Meteorology, University of Reading, Earley Gate, PO Box 243, Reading RG6 6BB, UK. (m.lockwood@reading.ac.uk)